

## Localized microwave heating in microwells for parallel DNA amplification applications

A. Kempitiya,<sup>1</sup> Diana A. Borca-Tasciuc,<sup>2</sup> Hisham S. Mohamed,<sup>3</sup> and Mona M. Hella<sup>1,a)</sup>

<sup>1</sup>*Department of Electrical, Computer and Systems Engineering, Rensselaer Polytechnic Institute, Troy, New York 12180, USA*

<sup>2</sup>*Department of Mechanical, Aerospace and Nuclear Engineering, Rensselaer Polytechnic Institute, Troy, New York 12180, USA*

<sup>3</sup>*Wadsworth Center, New York State Department of Health, Albany, New York 12201, USA*

(Received 5 December 2008; accepted 10 January 2009; published online 10 February 2009)

This work explores the potential of microwave heating for applications requiring parallel DNA amplification platforms. Device characterization and thermal modeling is performed on 4.1  $\mu\text{l}$  microfluidic chamber fabricated in polycarbonate. Microwave power at 6 GHz is delivered to the chamber via copper transmission line in a microstrip configuration. Microwave power reflection coefficient and temperature measurements are performed to characterize the power coupled to the chamber and rate of change in temperature. Temperatures up to 72 °C are achieved with less than 400 mW power applied at the input of the transmission line. Initial heating and cooling rates measured experimentally are  $\sim 7$  and  $\sim 6$  °C/s, respectively. These results suggest that microwave heating is an efficient, rapid heating technique suitable for programmable, parallel DNA amplification platforms to be employed in future genetic analysis systems. © 2009 American Institute of Physics. [DOI: 10.1063/1.3078273]

Polymerase chain reaction (PCR) has numerous medical applications from the detection of infectious diseases and pathogens to the identification of genetic fingerprints and mutations that cause hereditary diseases. Conventional PCR employs high cost, bulky equipment that provides slow heating rates and is both time consuming and labor intensive. In the past decade, miniaturized PCR systems have emerged as faster, low power consumption devices that could provide portability at a low cost. These systems typically employ contact-mediated heating methods using embedded resistive or Peltier elements.<sup>1-3</sup> However, the thermal-cycling rate is limited by the absolute thermal mass of the heating element itself. Furthermore, microheaters provide fixed temperature profiles optimized individually for a single specimen making multiplexing particularly difficult. More recently, noncontact heating methods, such as IR light<sup>4</sup> and laser, hot air,<sup>5</sup> and microwave radiation,<sup>6-8</sup> have been investigated for PCR applications. Among these techniques, microwave heating has significant advantages. This method is typically fast and very efficient because heating can be made spatially selective by confining the electromagnetic field within the PCR solution. Moreover, since heat generation takes place uniformly, the temperature of the solution is usually more uniform as compared to that obtained in systems employing contact-mediated heating. Microwave heating can be easily controlled via both frequency and signal strength, which provides higher flexibility in changing the temperature profile for different specimens or different genetic targets. Previous work has shown that large-scale microwave-based PCR systems can reach same efficiency as conventional PCR, while maintaining intact polymerase activity.<sup>6</sup> All these features make microwave heating of particular interest for

applications calling for fast, parallel amplification of multiple DNA targets on a single platform.

The first step toward developing integrated parallel DNA amplification and detection platforms is to better understand the requirements associated with microwave systems for localized heating as well as their limitations. Previous work suggests that this heating method is very efficient, producing  $\sim 1$  °C temperature rise per milliwatt power applied at 15 GHz.<sup>8</sup> However, this performance was obtained for a low temperature range, up to 32 °C,<sup>8</sup> where heat losses to ambient are less significant. More studies are needed to better understand equipment requirements to provide and maintain higher temperatures, to identify the most appropriate heating regime (transient versus steady state), and to determine the associated heating and cooling rates.

This work investigates the performance of microwave heating in microfluidic systems on a high temperature range, up to  $\sim 70$  °C. The proof-of-concept device, consisting of a 4.1  $\mu\text{l}$  test chamber integrated with a microwave transmission line was fabricated and tested. The thermal response of the test liquid is recorded as function of the applied microwave power for prolonged periods of time. Finite element modeling of transient heat transfer is carried out to assess the microwave power converted to dielectric heating and temperature uniformity within the heated liquid.

Figure 1 shows a schematic and a picture of the microwave heating module, which consists of a microfluidic well integrated with a microstrip transmission line. The well has a diameter of 2.3 mm and was drilled in 1 mm thick polycarbonate substrate. Both the transmission line and the ground plane (which covers the entire bottom side of the substrate) were made of 130  $\mu\text{m}$  thick copper. The dimensions of the transmission line were determined based on electromagnetic simulations using an equivalent circuit model as discussed previously.<sup>9</sup>

<sup>a)</sup>Author to whom correspondence should be addressed. Electronic mail: hellam@ccse.rpi.edu.

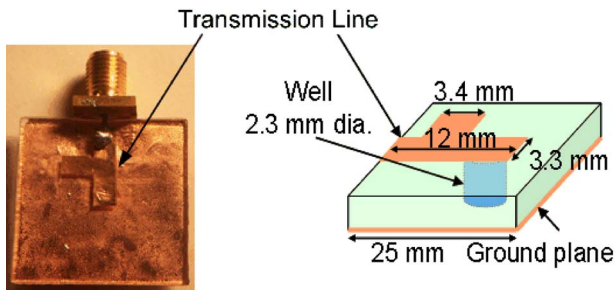


FIG. 1. (Color online) Device schematic.

The experimental setup for the evaluation of the temperature rise as well as heating/cooling rates uses an Agilent E8257D function generator in conjunction with Hittite 590LP5 linear power amplifier to generate the signal input into the transmission line. The performance of the system was tested employing water, which is the base liquid for most biological specimens. The device shown in Fig. 1 was flipped upside down and the well was filled with water using a syringe through a small insertion made into the ground plane. A 300  $\mu\text{m}$  fiber optic temperature sensor from FISO was used to measure the temperature rise during heating. The uncertainty of the temperature measurement is  $\pm 0.3$   $^{\circ}\text{C}$ . The tip of the fiber was positioned into the center of the well through the same insertion used for liquid filling. Teflon tape was wrapped carefully around the fiber optic sensor to provide a tight fit. This also helped reduce the water evaporation during heating. The power was manually switched on and off while the temperature was automatically recorded. To characterize the power level of the microwave signal coupled to the transmission line, the transmission coefficient of the microwave signal (S11) was measured using an Anritsu 37397C vector network analyzer. An S11 of  $-20.49$  dB was measured at 6 GHz at room temperature, indicating that more than 99% of the microwave power is coupled to the input of the transmission line when the well is fully filled with water.

Figure 2 shows the experimental temperature change as a function of time for four different power levels applied to the transmission line. As seen in Fig. 2, the initial heating rate is very fast at  $\sim 7$   $^{\circ}\text{C}/\text{s}$ . During the initial heating stage, the temperature is controlled by the heating of the microfluidic well, which has a relatively small thermal mass, and temperature increases rapidly. However, after the initial rapid heating, it is observed that the heating rate decreases signifi-

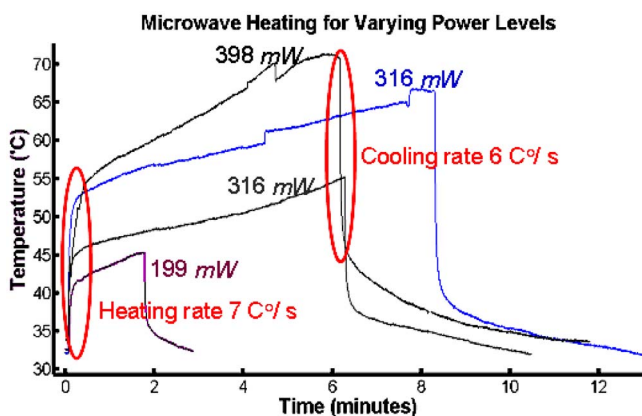


FIG. 2. (Color online) Temperature variation vs time at different microwave power levels.

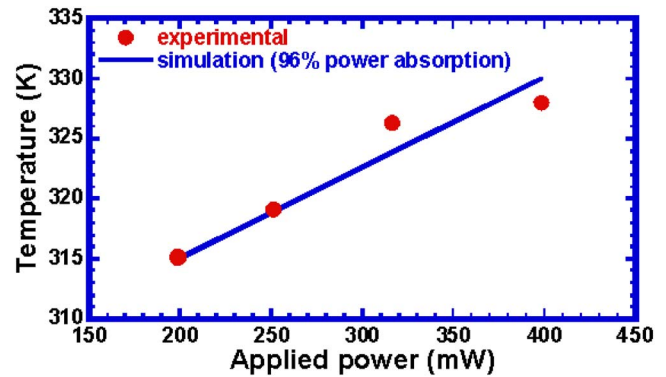


FIG. 3. (Color online) Experimental and simulated temperature rise as function of applied power.

cantly. In this regime, the substrate of the device, which has a much larger thermal mass, continues to absorb energy, and controls the temperature rise, slowly warming up. Similar trends are observed for cooling. The maximum temperature rise during the fast heating regime was  $\sim 55$   $^{\circ}\text{C}$ , measured  $\sim 8$  s after applying an input power of 398 mW to the transmission line. After 6 min of heating at this power level, the measured temperature increased to 72  $^{\circ}\text{C}$  (corresponding to a heating rate of less than 0.1  $^{\circ}\text{C}/\text{s}$ ).<sup>10</sup> These data indicate that microwave heating can efficiently heat up small liquid volumes, while having limited impact on the device substrate if used in the appropriate heating regime. However, to take full advantage of this heating technique, it will have to be implemented with *in situ* temperature monitoring, able to directly measure the temperature of the liquid, and an appropriate control system to adjust the input microwave power as required.

Finite element transient heat transfer modeling was performed to backout the amount of heating power absorbed by the water in microfluidic well and determine the spatial distribution of the temperature surrounding the well. A geometrical structure similar to the one shown in Fig. 1 was used for heat transfer modeling. Standard properties for water, copper, and polycarbonate were used, while convective heat transfer coefficient was approximated as 10  $\text{W}/\text{m}^2\text{K}$ . However the thickness of 200  $\mu\text{m}$  was used for both transmission line and ground plane due to geometrical size limitations in the finite element modeling (FEM) software (ABAQUS). This approximation could lead to overestimating heating losses. On the other hand, radiation heat losses from the device surface were neglected. The model assumed uniform heat generation rate inside the well during microwave heating. To estimate the percentage of absorbed power (microwave power converted to dielectric heating), the heat generation rate of the liquid was adjusted until the average temperature agreed reasonably with experimental temperature obtained for four different power levels, 24 s after heating was applied. The representative time (24 s) was chosen to be toward the end of the fast heating rate regime, which might be used to cycle the temperature in a real device.

Figure 3 shows the measured and predicted temperature at 24 s after the power was applied to the chamber. When the chamber is assumed fully filled with water, the simulated temperature rise and experimental data agree well when considering that  $\sim 96\%$  of the applied microwave power to the transmission line is converted to dielectric heating. A high

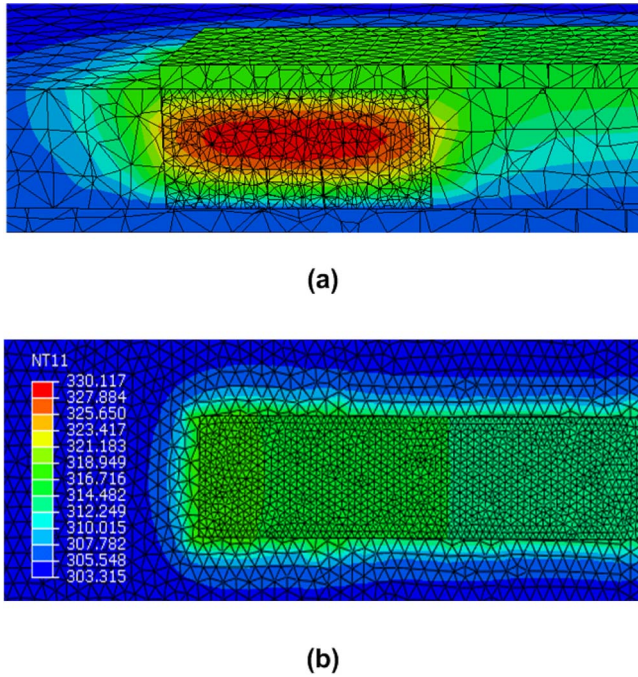


FIG. 4. (Color online) Temperature distribution in the microfluidic chamber and device substrate (a) cross section along the middle of the transmission line; (b) top view.

efficiency of energy conversion from electromagnetic to dielectric heating is expected. Overall efficiency of conventional microwave heating systems is very high, usually more than 80%.<sup>10</sup> In addition, with current device configuration the microwave energy is also confined in the well, which further reduces losses. The difference between input and absorbed power may come from Ohmic losses in the transmission line. However, the absorbed power may be less than 96% if air bubbles are present in the well. Trapped air gathers at the upper most surface, which for current experimental setup configuration is the ground plane. In the worst case scenario, the ground plane is thermally insulated from heated water. In this case, the heat loss from the well is significantly smaller and less absorbed power is needed to reach the experimentally measured temperature rise. Simulations of this case indicated that the absorbed power drops to  $\sim 40\%$  of the applied power.

Figure 4 shows the simulated temperature profile along the middle of the transmission line, 24 s after heating starts. The heating power density applied to the water in the microfluidic chamber is  $9.2 \times 10^7 \text{ W/m}^3$  (corresponding to 96% of

398 mW input power). The temperature of the liquid is uniform over more than 50% of the chamber. The temperature gradients occur mainly in the cross-plane direction of the device indicating the importance of heat losses through the copper electrodes. Thinner electrodes of lower thermal conductivity may be employed in future designs to improve the temperature uniformity. The temperature affected region of the substrate was also quantified in order to assess the optimum spacing of adjacent wells. For present device configuration, the temperature rise in the substrate becomes negligible at a distance of  $\sim 1 \text{ mm}$  from the transmission line, as seen from Fig. 4(b). These results indicate that it is critical to perform full thermal analysis of parallel DNA amplification platforms to ensure that temperature in each well is highly uniform and minimally affected by neighboring wells or transmission lines.

The proof-of-concept microwave heating device presented in this work was able to achieve fast heating and cooling rates of  $\sim 6\text{--}7 \text{ }^\circ\text{C/s}$ , and temperatures up to  $70 \text{ }^\circ\text{C}$  for an applied microwave power less than 400 mW. Thermal modeling has shown a relatively uniform heating profile within the liquid. The proposed system can be implemented in parallel DNA analysis and amplification platform, which have numerous applications from biological surveillance problems such as genetic analysis, population studies, and biothreats, to genetic studies in environmental sciences.

<sup>1</sup>Z. Zhan, C. Dafu, Y. Zhongyao, and W. Li, *First Annual International Conference On Microtechnologies in Medicine and Biology*, 2000, Vol. 1, p. 25.

<sup>2</sup>V. P. Iordanov, J. Bastemeijer, A. Bossche, P. M. Sarro, M. Malatek, I. T. Young, G. W. K. van Dedem, and M. J. Vellekoop, *IEEE Proceedings on Sensors*, 2003, Vol. 2, p. 1045.

<sup>3</sup>K. Shen, X. Chen, M. Guo, and J. Cheng, *Sens. Actuators B* **105**, 251 (2005).

<sup>4</sup>R. P. Oda, M. A. Strausbauch, A. F. Huhmer, N. Borson, S. R. Jurens, J. Craighead, P. J. Wettstein, B. Eckloff, B. Kline, and J. P. Landers, *Anal. Chem.* **70**, 4361 (1998).

<sup>5</sup>W. Wang, Z. X. Li, Y. J. Yang, and Z. Y. Guo, *17th IEEE International Conference on (MEMS) Micro Electro Mechanical Systems*, 2004 (unpublished), p. 280.

<sup>6</sup>C. Fermer, P. Nilsson, and M. Larhed, *Eur. J. Pharm. Sci.* **18**, 129 (2003).

<sup>7</sup>K. Orrling, P. Nilsson, M. Gullberg, and M. Larhed, *Chem. Commun.* **2004**, 790.

<sup>8</sup>J. Shah, S. G. Sundaresan, J. Geist, D. R. Reyes, J. C. Booth, M. V. Rao, and M. Gaitan, *J. Micromech. Microeng.* **17**, 2224 (2007).

<sup>9</sup>P. Garg, M. Hella, D. Borca-Tasciuc, and H. Mohamed, *Technical Proceedings of the 2008 Nanotechnology Conference*, 2008, Vol. 3, p. 577.

<sup>10</sup>R. J. Meredith, *Engineers' Handbook of Industrial Microwave Heating* (Institution of Electrical Engineers, 1998), Chap. 5.